

Pixel Detector Description for Simulation for the ATLAS Technical Proposal

D. Bintinger, K. Einsweiler and M. Gilchriese
Lawrence Berkeley Laboratory

P. Delpierre, A. Fallou, G. Hallewell and T. Mouthuy
Centre de Physique des Particules de Marseille

(1) Introduction

The purpose of this note is to provide a description of the ATLAS pixel detector system so that the pixel detectors may be adequately represented for physics simulations using DICE and ATRECON. It is understood that the design of the pixel system is at a very early stage. While studies of pixel module designs and the overall mechanical design are still under way, it is nevertheless possible to define the dimensions and other properties of a generic pixel system that are suitable for the simulation needs in preparation of the technical proposal. As the design progresses further, updated simulation geometry descriptions will be released so that the pixel detectors may be adequately represented for future physics simulations.

(2) Basic Layout and Pixel Size

The basic dimensions of the pixel system proposed to be implemented in the simulation are given in table (1) below. Alternative layouts are under investigation but the simulation results obtained with the basic layout should be applicable to other layouts. Detector positions and pseudorapidity coverage assumes a 2σ beam size of ± 10.6 cm.

(2.1) Basic dimensions of the proposed pixel layout.

The pixel system general layout is shown schematically in fig (1). In the barrel region, the radial dimension corresponds to the mean radius of the active detector element, and the half-length represents the distance from the IP to the edge of the active region. In the disk region, the z dimension corresponds to the mid-point between active elements that alternate on either side of the disk structure. The offset of these elements from the mid-point is 0.2 cm. The disk radial dimensions correspond to circles defining the inner and outer edges of the active region. Each disk is made up from 104 wedge-shaped tiles.

The nominal pixel size in the barrel region is $50\mu\text{m} (\phi) \times 300\mu\text{m} (z)$, although other pixel sizes are under consideration [1]. The nominal pixel size is the same for all barrel layers. The nominal pixel size in the disk region is also $50\mu\text{m} (\phi)$ and $300\mu\text{m} (r)$. The pixels in the disk region are not truly radial. The precise layout is described in the section on disk modules below.

Table (1) Nominal Pixel Layer Dimensions and Positions

Barrel Region	Nominal Radius (cm)	Active Half length (cm)	Number of Ladders
B-physics layer	4.0	35.04	16
First layer	11.50	35.04	45
Second layer	16.50	41.42	65
Disk Region	Nominal Z (cm)	Active Inner Radius (cm)	Active Outer Radius(cm)
	49.92	11.45	21.25
	55.40	11.45	21.25
	79.90	11.45	21.25
	85.00	11.45	21.25

(2.2) Barrel Modules

For the purposes of the simulation only, we use the following dimensions and properties for a barrel module, shown in fig (2):

- thickness of detector substrate: 150 μ m;
- thickness of bonded electronics: 75 μ m;
- total length (Z): 6.28 cm;
- total width (R- ϕ): 2.26cm;
- active length (Z): 6.18cm;
- active width (R- ϕ): 1.66cm;

Each ladder is an array of modules laid end to end. For easier mounting and modularity, there is no z overlap between modules in a ladder. A gap in z of 1mm is left between adjacent modules. Allowing an inactive interval of 0.5 mm at the end of each module (taken up by the guard ring structure, with some reserve for detector dicing), the total dead area in z between adjacent modules is 2 mm.

Detector layers are made up of axial ladders arranged in a "barrel stave" assembly. The number of ladders around the circumference of each layer are shown in table (1). With this modularity, the angles between the planes defining the polygon of detector ladders and the layer circumferences are 11.5°, 10.0° and 9.7° for the B physics layer and the layers at 11.5 cm and 16.5 cm respectively, with corresponding geometric overlaps in r- ϕ of 0.52°, 0.13° and 0.14°. The intended minimum active area overlaps in ϕ are about 0.3 mm, or 6 pixel rows.

(2.3) Disk Modules

Each disk is a polygon of overlapping pixel disk modules (wedges). The wedge modules overlap and alternate front and back with cooling and support in between them. Other services are

located on the outboard edges of the wedges. There are 104 overlapping wedges in one disk; 52 on the front and 52 on the back. The spacing in z between the two overlapping planes of wedges (active silicon to active silicon) is taken to be 0.4 cm. A drawing of a typical module (front and back wedge) is given in fig (3). The pixels within a wedge are arrayed as shown in fig (3). A front and back wedge pair forms one of the 52 trapezoids that form a disk. There is approximately a three pixel overlap at the center of the trapezoid formed by a front and back wedge [see fig (3)] and also at the edges with an adjacent trapezoid. The long dimension of a pixel is parallel to a radius at the center of a trapezoid but not at its edges since the pixels are arrayed in a rectangular pattern.

(3) Resolution

Since several pixel electronic readout schemes (analog and digital) are still under investigation for the high luminosity LHC application, the ultimate readout resolution is not yet decided, and may be different, for example, in the B physics vertexing layer to the other layers. Table (2) shows the intrinsic resolution achievable with "binary" ($s/\sqrt{12}$) and analog readout. For layers equipped with binary readout, a conservative goal for the ϕ resolution is $\pm 18 \mu\text{m}$, including alignment and positioning systematics. In the orthogonal direction (z for cylinders, r for disks), a conservative value for the resolution is $(300\mu\text{m}/\sqrt{12}) = \pm 87 \mu\text{m}$.

With analog readout, an intrinsic ϕ resolution of better than $\pm 7 \mu\text{m}$ is achievable [3,4], which when combined with the alignment and positioning precision of $\pm 7 \mu\text{m}$, will give an overall spatial resolution in ϕ of $\pm 10 \mu\text{m}$. The resolution in z,r will depend on the track incidence, and the crossing point along the $300 \mu\text{m}$ pixel dimension. Previous pixel resolution studies [3,4] have shown that the end regions along the pixel long dimension have enhanced resolution - through charge sharing - relative to the central regions, whose resolution is "binary". Fig (4a) illustrates the regions of high and low z,r resolution. We assume that the end $25 \mu\text{m}$ of one pixel shares charge with the end $25 \mu\text{m}$ of the next to give an enhanced resolution of $10 \mu\text{m}$ over an effective area $50 \mu\text{m} \times 50\mu\text{m}$. Binary resolution is assumed in the remaining $250 \mu\text{m} \times 50 \mu\text{m}$ central zone. By weighting the relative areas of the zones of high and low resolution in z,r , we find a weighted z,r resolution of $62 \mu\text{m}$ for the case of analog readout.

A pixel tiling scheme ["bricking": fig (4b)], with adjacent ϕ rows of pixels shifted in z by half a pixel length ($150 \mu\text{m}$) will exploit lateral (ϕ) charge sharing (perhaps aided by E^B effects) to further improve the z resolution. An estimate of the z,r resolution is $43 \mu\text{m}$, assuming there is always charge sharing in ϕ , but ignoring any z,r charge sharing. This value is equal to twice the binary z,r precision for the unbricked case. Taking full account of z,r charge sharing with bricking, we find a second effective $50 \mu\text{m}$ zone with $10 \mu\text{m}$ resolution, and two $100 \mu\text{m} \times 50 \mu\text{m}$ zones with binary resolution. By weighting the relative areas of the zones of high and low resolution in z,r , we find a weighted z,r resolution of $23 \mu\text{m}$ [table (2)], which probably represents the best z,r resolution achievable.

Since detailed studies of resolution, including the case of a "bricked" array of pixels in the ATLAS geometry have yet to be made in test beams, we have proposed for the purposes of simulation for the technical proposal pixel intrinsic resolutions of $15 \mu\text{m}$ (ϕ) and $87 \mu\text{m}$ (z,r) for the case of binary readout, and $7 \mu\text{m}$ (ϕ) and $43 \mu\text{m}$ (z,r), in the case of analog readout with bricking, as indicated in table (2).

Table (2) Intrinsic Resolution of Pixels with Binary and Analog Readout.

	Binary (s/ $\sqrt{12}$)	Analog	Analog + Bricking
$\sigma(\phi)$	15 μm^*	7 μm	7 μm^*
$\sigma(z,r)$	87 μm^*	62 μm	43 * - 23 μm

(4) Radiation Lengths

The material (X/X_0) breakdowns for the B physics (4 cm radius) and high luminosity (11.5 & 16.5 cm) barrel and the disk pixel tile modules, assuming normal incidence, are shown in table (3). The effects of electronics, cooling, cabling and support are averaged over the whole tile area (example: 62.8 x 22.6 mm for barrel pixel tiles) but do not include factors to take account of the overlap in azimuth between adjacent tiles.

Table (3) Radiation length (% X/X_0) contribution from pixel module components, [NO OVERLAP: see text]

Component	Barrel Pixel Modules (4 cm B physics layer)	Barrel Pixel Modules (11.5, 16.5 cm layers)	Disk Pixel Modules
(1) Silicon detectors	0.16	0.16	0.38 (det.+elec.)
(2) Electronics + bump bonding	0.14	0.14	incl. in (1)
(3) Cooling tube	incl. in (5)	incl. in (5)	incl. in (4)
(4) Support	0.11 (contr. of external support shell in Be)	0.11 (contr. of external support shell in Be)	0.14 (in Be +tube in Be)
(5) Cooling (average)	0.17 (liquid film, + tube in Be)	0.24 (liquid film, + tube in Al)	0.17 (Water)
(6) Cabling (average)	0.14	0.14	0.14
(7) Module attachments (average)	0.18	0.18	0.00 (not used)
TOTAL	0.90	0.97	0.83
TOTAL Exc. Indiv. Be Support Shells	0.79	0.86	

Table (3) effectively assumes that the module dimensions will be used in the simulation, which will naturally calculate the overlap factor. If this is not the case, the radiation lengths for the barrel layers at 4 cm, 11.5 cm and 16.5 cm should be increased to take account of azimuthal overlaps occurring;

(a) between the "full depth" regions (*which include the detector substrate, readout and cabling, plus contributions from all the support elements except for the external beryllium support cylinder*) of tiles in a ladder, and the tiles in an adjacent ladder. The full depth regions are 2.06 cm wide, and include an insensitive zone occupied by the pixel column sparsification and time stamping logic along the outboard 2 mm of each row of readout chips [fig. (2)]. These regions have effective radiation length 0.77% X/X_0 (4 cm layer) and 0.92% X/X_0 (11.5 & 16.5 cm layers):

(b) between the 1 mm peripheral "substrate depth" zone [0.16% X/X0: fig. (2)] along the edges of tiles in a ladder, and the tiles in an adjacent ladder:

The contributions of (a) and (b) need to be considered separately.

In the case of (a), the X/X0 contribution is itself the sum of two components: an "active area / active area" overlap (to avoid dead zones at the ladder boundaries) and a "column logic / active area" overlap. The radiation length contribution of the active angular overlap depends on the ratio of the angular overlap between adjacent ladders (shown in § 2.2 for each layer) to the fractional layer circumference subtended by the active width of a ladder. The radiation length contribution of the column logic overlap may be represented to a reasonable approximation by the ratio of the 2 mm width of the column logic zone to that of the 22.6 mm tile width. This contribution is the same for all three layers.

In the case of (b), the X/X0 contribution of the "substrate depth" overlap is given approximately by the ratio of overlap width of the 1 mm wide inactive zone and the 22.6 mm tile width. This contribution is the same for all three layers.

As an example for the 4 cm layer (with 16 circumferential ladders),

(a) Full depth overlap X/X0 contribution = $0.79\% \times [\{0.52^\circ / (360^\circ/16)\} + (2.0/22.6)] = 0.088\%$

(b) Substrate depth overlap X/X0 contribution = $0.16\% \times (1.0/22.6) = 0.007\%$

To the contributions from (a) and (b) needs to be added the 0.77% base X/X0 contribution [Table (4)]. The corresponding base contribution for the 11.5 and 16.5 cm layers is 0.92%. The material presented by the overall Be layer support shell (0.12% X/X0) must finally be added to the sum of the base material and the two overlap factors to give the overall material.

Table (4) Radiation Lengths of the Barrel Pixel Layers, Including Overlap

Layer Radius (cm)	Base X/X0 (no overlap) (%)	Overlap Addition (%)	Total (inc 0.11% X/X0 Be support shell)
4.0	0.79	0.095	1.00
11.5	0.86	0.097	1.07
16.5	0.86	0.105	1.08

For the forward pixel disks, X/X0 increases to 0.99%, taking overlap into account.

A plot of radiation lengths vs rapidity is given in fig (5) [fig (6)] for the system without [with] the B-physics layer. Module overlap is taken into account. It is premature to put in azimuthal X/X0 dependence, although it will surely exist.

The design of the pixel mechanical structure, cooling and electrical services is at a very early stage. To facilitate simulations in which module overlap is calculated automatically from the module geometry, table (5) summarizes the present estimate of total radiation lengths for various cylindrical and disk elements of the pixel system. Components of the B-physics layer are listed separately. Radiation lengths are ϕ averaged, and (r,z) dimensions of elements are shown.

Table (5) Total Radiation Length* (%X/X0 at normal incidence) for each cylinder and disk element of the Pixel System. The B-physics layer components are listed separately.

**For simulations which calculate module overlap automatically from module geometry.*

Cylinder Elements

Radius (cm)	Z-start (cm)	Z-end (cm)	Total Percent X/X0	Element	Active/Dead Material
4.00	0.00	35.04	0.79	B pixel layer	A+D
5.00	0.00	45.00	0.11	B layer Be Support shell	
5.05	35.04	45.00	0.17+0.30	B layer: cooling, cabling	D
5.05	35.04	45.00	0.24	Be Cyl: Be end Reinforc. ring	D
11.5	0.00	35.04	0.92	11.5cm pixel layer	A+D
12.5	0.00	45.00	0.11	11.5 cm layer Be Support shell	D
12.55	35.04	45.00	0.24+0.30	11.5 cm layer cooling, cabling	D
12.55	35.04	45.00	0.24	Be Cyl: Be end Reinforc. ring	D
16.5	0.00	41.42	0.92	16.5cm pixel layer	A+D
17.5	0.00	45.00	0.11	16.5 cm layer Support shell	D
17.55	35.04	45.00	0.24+0.30	16.5 cm layer cooling, cabling	D
17.55	35.04	45.00	0.24	Be Cyl: Be end Reinforc. ring	D
22.5	0.00	45.00	0.30	Overall cylind. Stiffener (in active volume*)	D
*Optional at this stage-engineering studies to see if this will be necessary					
22.5	45.00	86.00	0.36	Outboard cylind. Support structure	D
22.5	45.00	86.00	0.07+0.07	B layer Outboard Cooling, cabling	D
22.5	45.00	86.00	0.39+0.37	Outboard Cooling, cabling (11.5,16.5 cm layers only)	D
22.5	49.92	55.40	0.11	cooling & cabling for 1st disk	D
22.5	55.40	79.90	0.22	cooling & cabling disks 1&2	D
22.5	79.90	85.00	0.33	cooling & cabling Disks 1, 2 & 3	D
22.5	85.00	86.00	0.44	cooling & cabling Disks 1, 2, 3 &4	D

Table (5) continued...

Disk Elements

Z (cm)	r-Inner (cm)	r-outer (cm)	Total Percent X/X0	Element	Active/Dead Material
49.92	11.4	21.3	0.68	1st Disk Layer	A+D
49.92	21.25	22.5	0.18	1st Disk Support + services	D
55.40	11.4	21.3	0.68	2nd Disk Layer	A+D
55.40	21.25	22.5	0.18	1st Disk Support + services	D
79.90	11.4	21.3	0.68	1st Disk Layer	A+D
79.90	21.25	22.5	0.18	1st Disk Support + services	D
85.00	11.4	21.3	0.68	1st Disk Layer	A+D
85.00	21.25	22.5	0.18	1st Disk Support + services	D
45.00	5.0	12.5	0.15+0.14	B layer B cooling , cabling	D
45.00	12.5	17.5	0.09+0.08	B layer B cooling , cabling	D
45.00	17.5	22.5	0.07+0.06	B layer cooling, cabling	D
45.00	12.5	17.5	0.22+0.23	11.5 cm and B layer cooling, cabling	D
45.00	17.5	22.5	0.545+0.43	16.5,11.5 cm and B layer cooling, cabling	D
45.00	5.00	22.5	0.36	Beryllium Spacer for cylinders	D
86.00	22.50	30.00	0.05	Spacer support- ing pixel system from strip support at r=30cm.	D

The pixel services must be routed through the gap between the silicon tracker and the first TRT disk. The approximate radiation length of these services is $(25\text{cm}/R) \times 0.89$ without the B-physics layer and $(25\text{cm}/R) \times 0.94$ with the B-physics layer. At the outermost radius these must be added to other services.

References

- [1] At CPPM, several pixel readout electronics geometries are under study. Of these, $50\ \mu\text{m} \times 300$ or $400\ \mu\text{m}$ are the most suitable for the LHC application. The present LBL readout design calls for a pixel size of $(50 \times 300)\ \mu\text{m}$.
- [2] Pixel Detector Back-up document ATLAS-INDET-NO -XXXX (December 1994)
- [3] J. Jernigan et al, "Preliminary Test Results from a Telescope of Hughes Pixel Arrays at FNAL" SLAC- PUB- 5925 (1992)
- J. F. Arens et al, "Progress Report of the Collaboration for the Development of Pixel Vertex Detector Technology"
SSC Pixel Detector Development Collaboration (Oct 1, 1992)
- [4] C. Kenney et al "A Prototype Monolithic Pixel Detector" Proc. 1st Intl. Symposium on Development and Application of Semiconducteur Tracking Detectors, Hiroshima (May 1993); Nucl. Instr. & Meth. A 342 (1994) 59

Figure Captions

Fig (1) Schematic layout of the ATLAS pixel system, showing the cylindrical and disk surfaces.

Fig (2) The geometry of a barrel pixel module, showing the placement of readout.

Fig (3) The geometry of a disk pixel module, showing the placement of readout.

Fig (4a) Illustration of the regions of enhanced spatial resolution possible in z (barrel layers) or r (disk layers) through charge sharing between the ends of adjacent pixels.
Analog readout of pixel charges.

Fig (4b) Illustration of a pixel "bricking" geometry, with adjacent pixel rows shifted by half a pitch in z (barrel layers) or r (disk layers). Charge sharing in ϕ produces an extra region of enhanced z, r resolution per pixel, in addition to charge sharing between the ends of adjacent pixels. Analog readout of pixel charges.

Fig (5) Overall radiation length of the material in the high luminosity layers of the ATLAS pixel detector.

Fig (6) Overall radiation length of the material in the ATLAS pixel detector (including the B-physics layer).

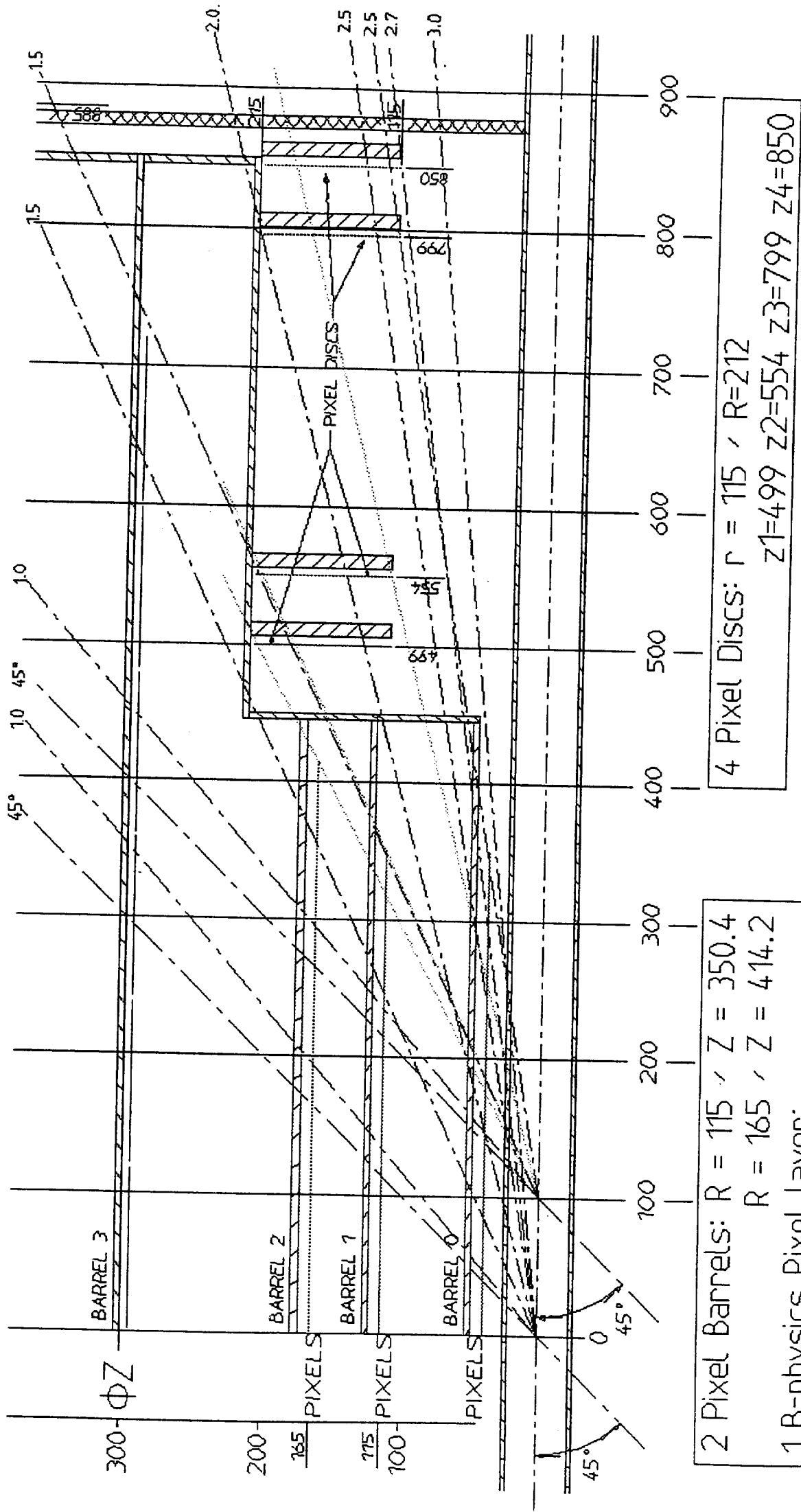
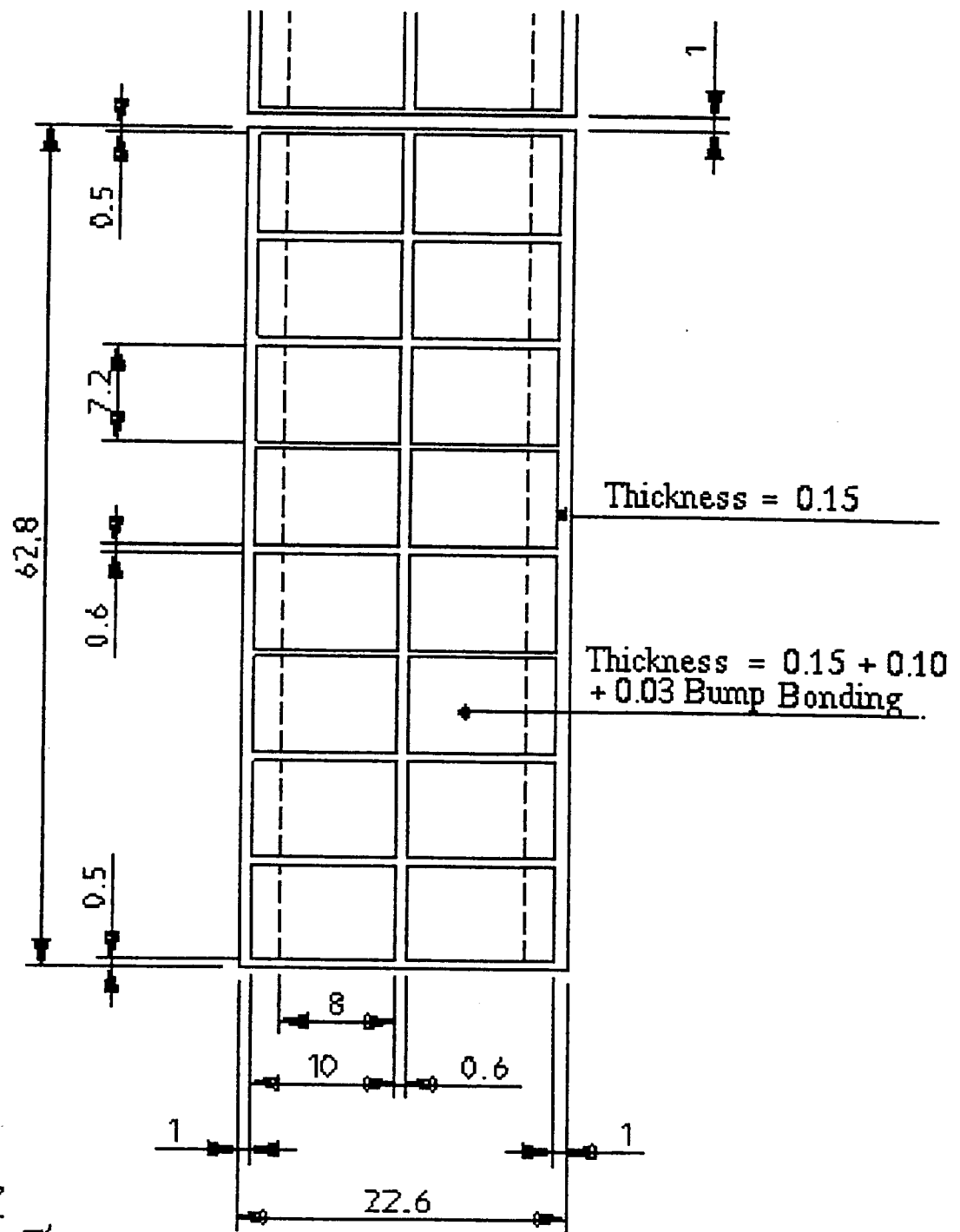


Fig (1)



8 Chips on Z
 2 Chips on $r\varnothing$
 24 Pixels (0.3mm) on Z / Chip
 160 Pixels (0.05mm) on $r\varnothing$ / Chip

Fig (2)

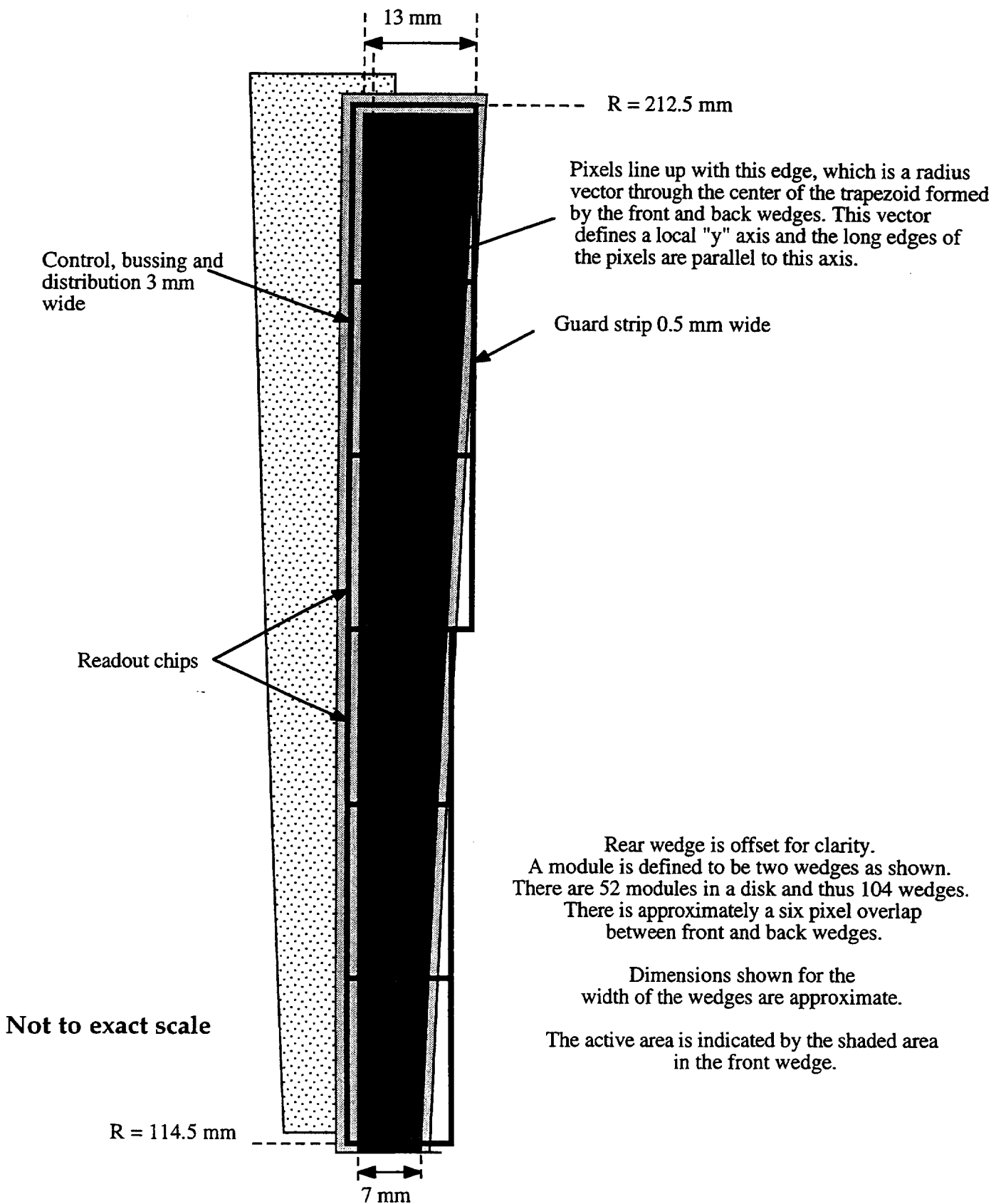
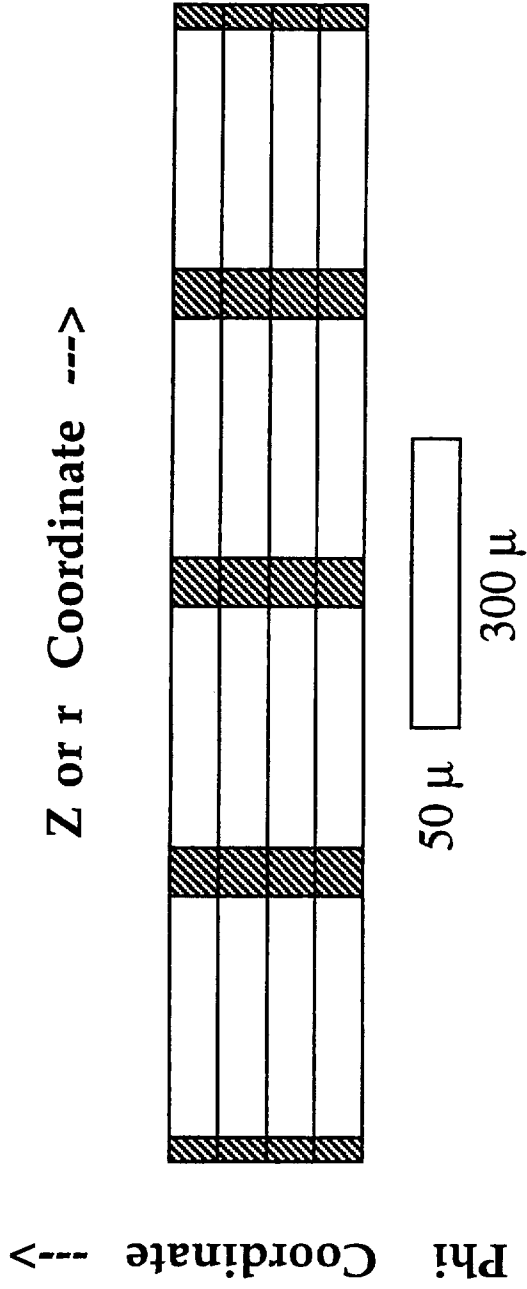


Fig (3)



Pixel Geometry

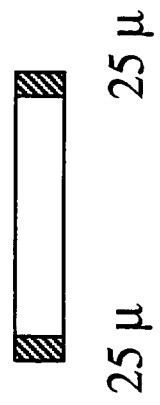


Fig (4a)

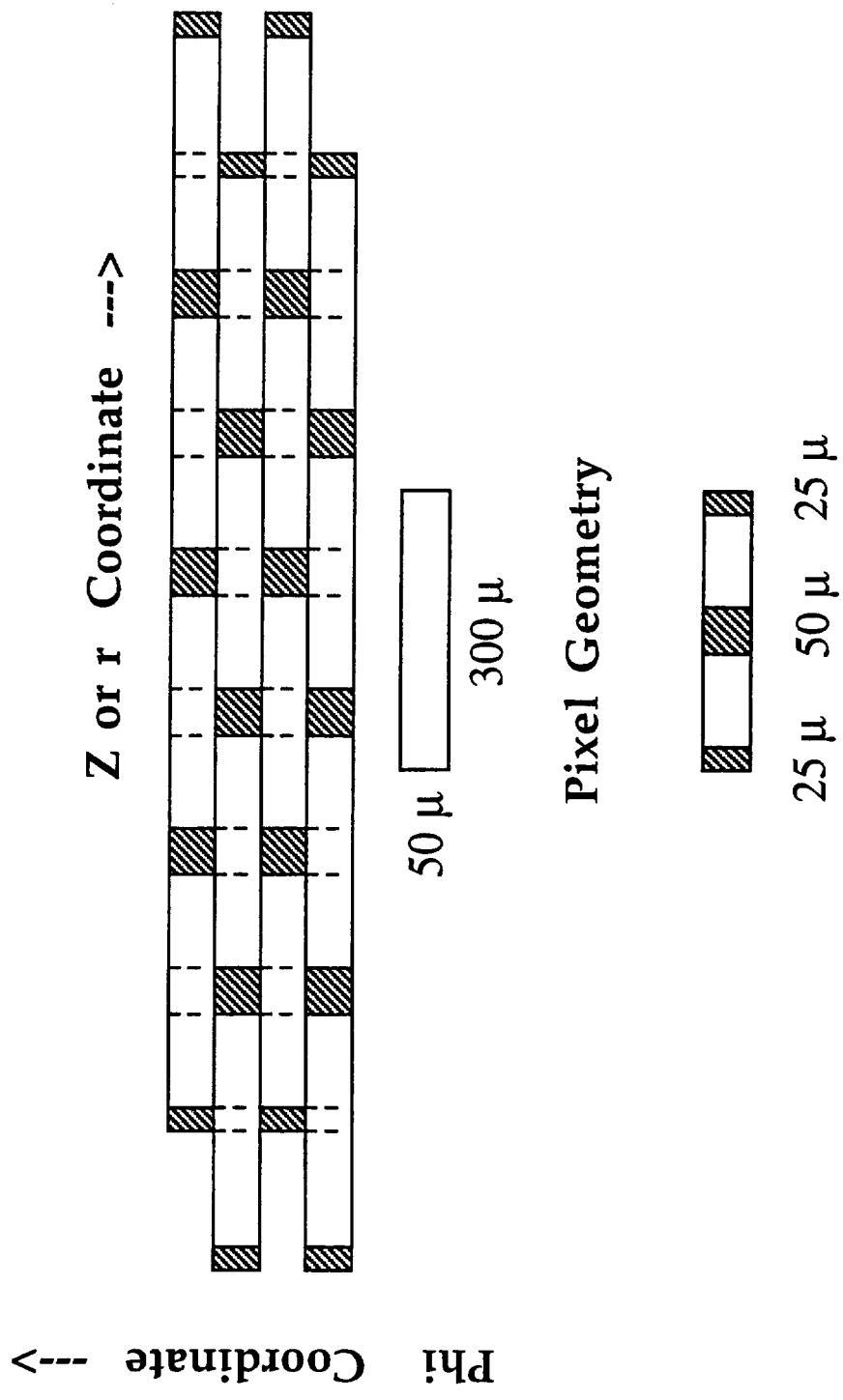
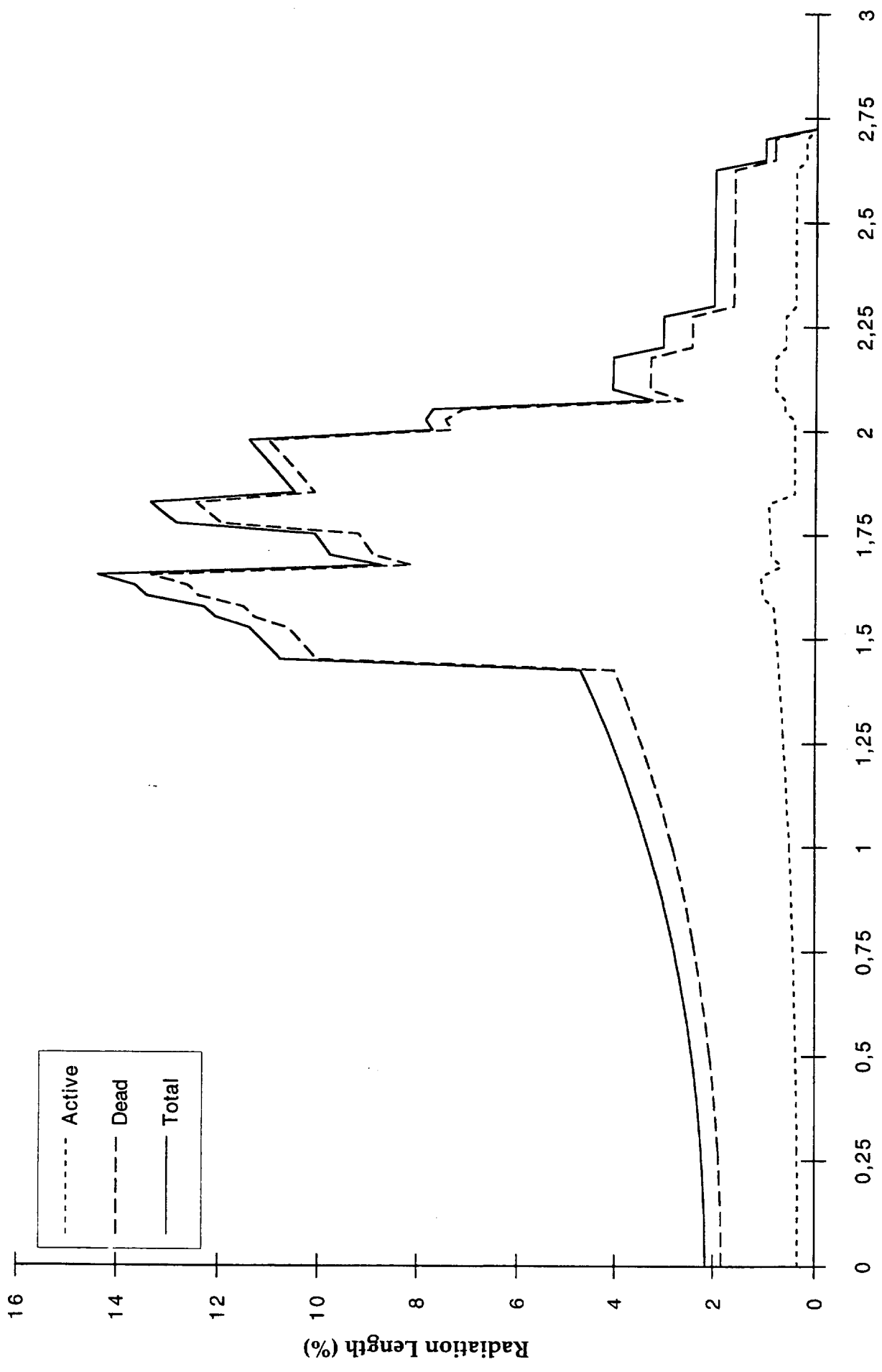
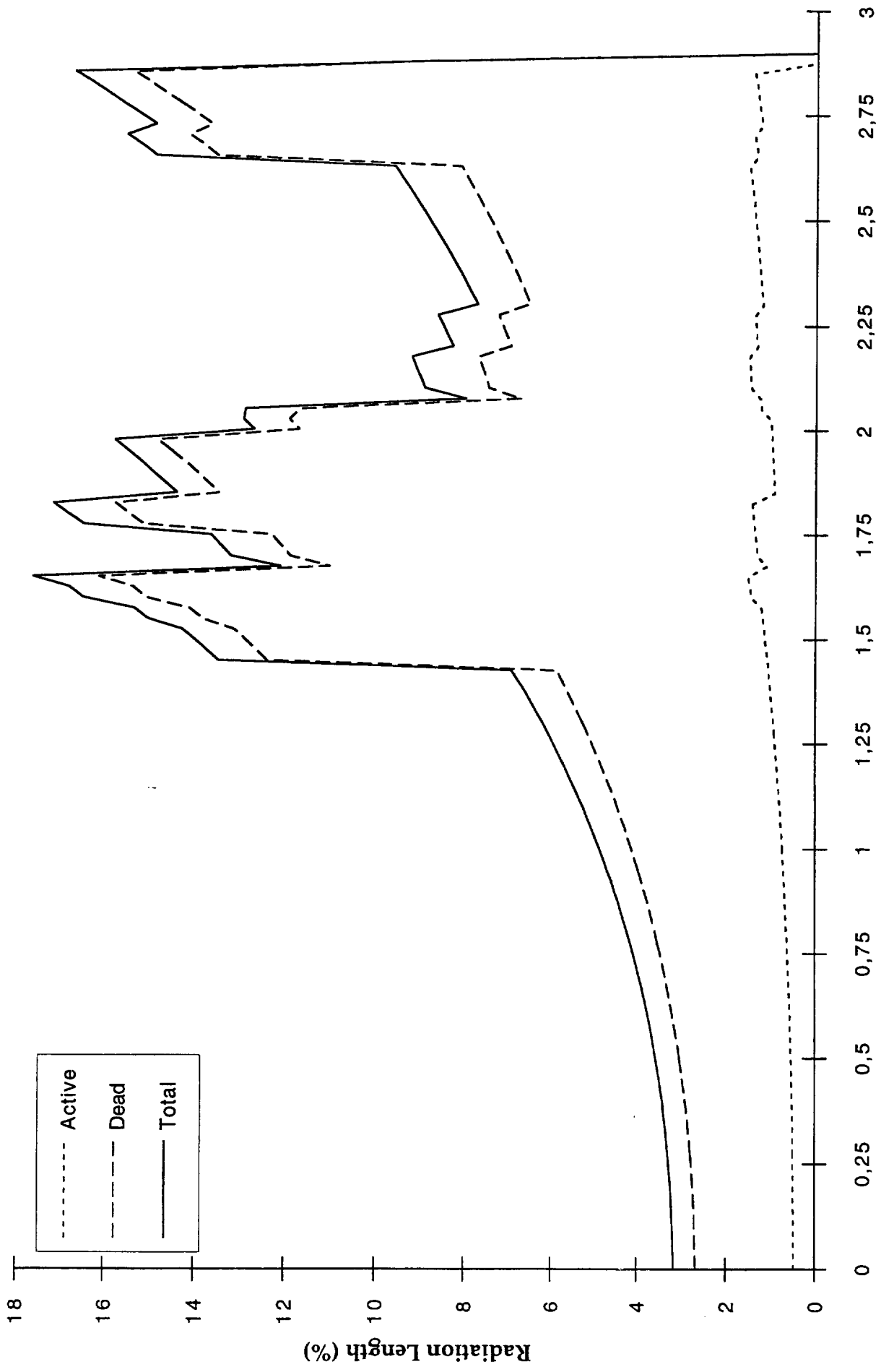


Fig (4b)



Pseudorapidity
Fig (5)



Pseudorapidity
Fig (6)

